Available online at www.sciencedirect.com
SCIENCE DIRECT®

Journal of the European Ceramic Society 24 (2004) 2417–2424
www.elsevier.com/locate/jeurceramsoc

Structural, elastic, thermophysical and dielectric properties of zinc aluminate ($ZnAl_2O_4$)

N.J. van der Laag[a], M.D. Snel[a], P.C.M.M. Magusin[b], G. de With[a,*]

[a]*Laboratory of Solid State and Materials Chemistry, Eindhoven University of Technology, PO Box 513, 5600 MB Eindhoven, The Netherlands*
[b]*Schuit Institute of Catalysis, Eindhoven University of Technology, PO Box 513,5600 MB Eindhoven, The Netherlands*

Received 1 March 2003; accepted 22 June 2003

Abstract

Dense zinc aluminate (gahnite) ceramics have been prepared at different sinter temperatures ranging from 1200 to 1600 °C from zinc aluminate powder prepared via the solid-state synthesis. A maximum achieved relative density of 93% was achieved. Several bulk properties like Young's modulus, heat capacity, thermal diffusivity and conductivity have been determined and estimations of the bulk properties at 100% density are made. Furthermore, in spinel-type materials like zinc aluminate the process of cation inversion occurs, which is in general not taken into account in computer simulations for the prediction of bulk properties. In order to determine whether the amount of cation inversion can be influenced by the preparation method resulting in different bulk properties, zinc aluminate powders were synthesised using solid-state synthesis, co-precipitation and a sol-gel method at different temperatures. The resulting powders were zinc deficient due to the volatile nature of zinc at the calcining temperatures. The cation inversion of these powders was investigated using solid-state MAS ^{27}A1 NMR indicating that the cation inversion is very small for pure zinc aluminate irrespective of the preparation method.

Keywords: Dielectic properties; Mechanical properties; Sintering; Spinels; Thermal properties; $ZnAl_2O_4$

1. Introduction

Zinc aluminate ($ZnAl_2O_4$), naturally occurring as the mineral gahnite, is a member of the spinel family. At present zinc aluminate is used as a catalyst for the dehydration of saturated alcohols to olefins,[1] methanol and higher alcohol synthesis,[2,3] preparation of polymethylbenzenes,[4] synthesis of styrenes from acetophenons,[5] and double bond isomerisation of alkenes.[6] Furthermore, zinc aluminate can also be used as a catalyst support, since it has a high thermal stability, low acidity and a hydrophobic behaviour. Moreover, it has a strong metal–support interaction preventing e.g. platinum and platinum/tin to sinter.[7] Finally, zinc aluminate can be used as a second phase in glaze layers of white ceramic tiles to improve wear resistance and mechanical properties and to preserve whiteness.[8]

Zinc aluminate is normally synthesised via a solid-state reaction of zinc and aluminium oxides above 800 °C[9,10] or via coprecipitation,[7,12] hydrothermal [11] and sol-gel methods with several organic precursors.[10,12–14] It could be used as a ceramic material similar to e.g. magnesium aluminate ($MgAl_2O_4$) and manganese–zinc ferrites [$(Mn,Zn)Fe_2O_4$]. However, in the literature only a few papers have been published about the sintering of zinc aluminate ceramics,[9,15–17] rendering many bulk properties, e.g. Young's modulus, unknown. In this paper, the preparation of dense zinc aluminate ceramics is reported and some of its elastic, thermophysical and dielectric properties are determined. Furthermore, attention is paid to the influence of preparation on cation inversion, which occurs in spinels. In predictions of the bulk properties using computer simulations this cation inversion is usually neglected. However, for a good comparison between experiment and simulation it is required to have information about the (small) cation inversion in zinc aluminate.

2. Crystallographic aspects of zinc aluminate

The crystal structure of spinel stricto sensu ($MgAl_2O_4$) has been independently determined by

* Corresponding author. Tel.: +31-40-247-2770; fax: +31-40-244-5619.
E-mail address: g.dewith@tue.nl (G. de With).

0955-2219/$ - see front matter © 2003 Elsevier Ltd. All rights reserved.
doi:10.1016/j.jeurceramsoc.2003.06.001

Bragg[18] and Nishikawa[19] in 1915. It has the space group F_{d3m} (O_h^7 number 227 in the International Tables [20]) and has a cubic structure made of eight molecular units (AB_2O_4). There are three main groups of compounds with the spinel structure and the chemical formula AB_2O_4. II–III spinels, IV–II spinels and defect-spinels. In the first group the A cation is divalent and the B cations trivalent. Magnesium aluminate and zinc aluminate are examples of this group. In the second group the A cation is tetravalent en the B cations divalent. Ülvospinel ($TiFe_2O_4$) is a well-known member of this group. Spinels from the third group have vacancies on sites where cations should be. A well-known example is γ-alumina. One unit cell of a compound with the spinel structure is built up from 32 oxygen atoms arranged in a fcc-lattice, giving 64 tetrahedral and 32 octahedral interstices. In a II–III spinel the divalent A cations occupy eight tetrahedral interstices and the trivalent B cations occupy 16 octahedral interstices. This distribution of the cations is designated as *normal*. However, this is thermodynamically not always the most stable situation, since the configurational entropy counteracts the site preference energy. Therefore, in spinels A and B cations may interchange interstices via diffusion, eventually leading to the limiting situation where all the A cations are in octahedral interstices. The latter situation is designated as *inverted*.

All distributions between the two extremes are possible and the degree of inversion is given by the inversion parameter x, which is defined as the fraction of A cations in octahedral sites. The inversion parameter x can be obtained via careful single crystal X-ray diffraction or via nuclear magnetic resonance with magic angle spinning (MAS–NMR). In the latter case x can be obtained for aluminates from the peak areas by:

$$x = \frac{2}{1 + (\mathrm{Al^{VI}}/\mathrm{Al^{IV}})}, \quad (1)$$

where Al^{VI} is the peak area of aluminium cations in an octahedral surrounding (~0–10 ppm) and Al″ of the aluminium cations in a tetrahedral surrounding (~60–70 ppm).

The inversion in zinc aluminate is known, by X-ray diffraction,[24–26] to be small in contrast to e.g. magnesium aluminate.[27] Moreover, in computer simulations the inversion of zinc and aluminium atoms is also found to be energetically unfavourable.[28,29] Furthermore, NMR studies on the cation inversion in zinc aluminate, which is prepared via the solid-state synthesis route, confirm the virtual absence of inversion.[30] However, inversion has been found to some extent in zinc aluminate synthesized using a sol-gel method with alkoxides depending on the temperature.[14]

3. Instrumentation

The structural properties of zinc aluminate powders were investigated by powder X-ray diffraction (XRD) on a Rigaku Geigerflex using Cu$K_{\alpha 1}$, radiation. One-dimensional solid state magic angle spinning ^{27}Al nuclear magnetic resonance (MAS ^{27}Al NMR) spectra were measured with a ~6 mg sample for quantitative comparison on a Bruker DMX500 spectrometer operating at an ^{27}Al NMR frequency of 130.32 MHz using a sample-rotation of 30 kHz. Rotor-synchronised echoes were recorded using the two-pulse sequence p_1–τ–p_2–τ–FID (Hahn spin–echo pulse [21,22]) with a dwell time (τ) of 1 μs and optimised pulse lengths p_1 and p_2 of 1.2 and 2.4 μs, respectively. A delay time of 10 s was applied between each of the 128 scans for a quantitative comparison between the samples. Variation of the delay time revealed that the peak areas Al^{IV} and Al^{VI} varied hardly or within the quatitative limit (<8%), respectively, at longer delay times than 10 s. The dielectric properties were determined on a HP 4284A LCR meter and the elastic properties with a Panametrics model 25DL, using the pulse–echo method.[23] The thermophysical properties as diffusivity and heat capacity were determined on a Compotherm XP/20X and on a Differential Scanning Calorimeter (DSC) of Perkin-Elmer model Pyris 1, respectively.

4. Preparation

4.1. Powder synthesis

Zinc aluminate was made via three different routes: solid-state synthesis, coprecipitation and a sol-gel method. In the solid-state synthesis route equimolar amounts of zinc oxide (Merck, >99%) and γ-alumina (Degussa) with a total weight of 90 g were put into a plastic container. Distilled water was added and the mixture was mixed. After evaporating most of the water overnight, the mixture was dried at 110 °C for 2 h and subsequently the large agglomerates were pulverised in an agate mortar. The mixture was divided in three batches, each put in an alumina crucible covered with an alumina lid in order to prevent contamination of the furnace with zinc. In separate experiments the batches were heated in air to 1000 °C for 8 h, 800 °C for 8 and 12 h, respectively, with a heating rate of 10 °C min^{-1}. The batches were dried (without the lid) for 1 h at 110 °C prior to the heating.

In the coprecipitation method, described in Ref. 12 an equimolar amount of zinc nitrate and aluminium nitrate (both from Merck, >99%) was dissolved in a citric acid solution of pH = 2 under stirring. A solution of 16 wt.% ammonia (Merck, >99%) was slowly added until the solution was neutral and a chelate was formed. The

chelate was dried in air for 20 h and subsequently dried in a furnace at 50 °C (68 h) and 110 °C (20 h). The resulting powder was divided into three batches.

As in the solid-state route, the batches were heated in air to 1000 °C for 8 h, 800 °C for 8 and 12 h, respectively, with a heating rate of 10 °C min^{-1}. Although the batches were put into an alumina crucible, this time the lid was removed in order to let the nitrogenous fumes evaporate. The batches were dried at 110 °C (1 h) and 300 °C (6 h) prior to calcining in order to remove the nitrates.

Zinc aluminate was synthesized using a sol-gel method based on the method described by Monrós et al.[31] Aluminium and zinc chloride (Merck, >99%) were dissolved in 100 ml water, resulting in an aluminium and zinc cation concentration of 0.6 and 0.3 M, respectively. Furthermore, 10 g of gelatin (Merck, >99%) is dissolved in 100 ml of water under stirring and heating to obtain a homogeneous solution. The warm gelatin solution was added to the cation solution under heating and stirring, until a homogeneous mixture was obtained, subsequently followed by cooling in a refrigerator (4 °C) for 30 min. The resulting gel was aged for 96 h at room temperature and dried at 80 °C for 40 h.

In order to burn out the gelatin, the dried gel was put in an alumina vessel and heated up to 400 °C at a rate of 3 °C min^{-1}, and kept at that temperature for 7 h in a gas flow of 80% N_2/20% O_2. After cooling down at a rate of 3 °C min^{-1}, the powder was ground and subsequently reheated at 3 °C min^{-1} to 800 °C. The zinc aluminate powder was kept at that temperature for 12 h in 80% N_2/20% O_2 gas mixture flow and, subsequently, cooled to room temperature at 3 °C min^{-1}. In an additional experiment this powder was reheated to 1000 °C at 10 °C min^{-1} and kept at that temperature for 8 h.

4.2. Compaction and sintering

Zinc aluminate powder prepared via the solid state route at 1000 °C for 8 h was ball-milled for 24 h with a small amount of isopropanol. Subsequently, the powder was sieved using a copper sieve with a mesh of 50 μm. Finally to improve compaction behaviour, a small amount of distilled water was added to the powder, before it was stored in a closed plastic container at 70 °C for 24 h.

The powder was put in a steel die with a diameter of 12 or 15 mm, which was lubricated with a 90% petroleum ether–10% oleic acid mixture, followed by uniaxially pressing to 70 or 150 MPa. The resulting tablets were put in an alumina crucible closed with an alumina lid, but were covered with extra zinc aluminate powder. The tablets were heated to different temperatures between 1200 and 1600 °C at 3 °C min^{-1} and kept at those temperatures for 8 h.

5. Results and discussion

5.1. Structural properties

XRD measurements showed that zinc aluminate powder (JCPDS file 05-0669) has been formed (see Fig. 1). However, in all samples zinc oxide (JCPDS file 36-1451) was present, except those calcined at 1000 °C and prepared via the sol-gel method. This is in agreement with the results from Keller et al.,[10] who found that at 1000 °C ~95% pure zinc aluminate results. The presence of θ- or δ-alumina, which would have formed when γ-alumina is heated to the applied temperatures,[32] or α-alumina was not detected in any sample. This indicates that the aluminium cations and oxygen anions form under presence of zinc oxide a spinel lattice.

5.2. Composition

The zinc–aluminium ratio of the single phase zinc aluminate prepared via the solid state route, coprecipitation and the sol-gel method at 1000 °C is determined using atomic absorption spectroscopy (AAS). The composition is $Zn_{0.95}Al_2O_4$, $Zn_{0.83}Al_2O_4$ and $Zn_{0.48}Al_2O_4$ (accuracy ±5%, aluminium and oxygen set to 2 and 4, respectively) for the solid state, coprecipitation and the sol-gel prepared zinc aluminate, respectively. The zinc–aluminium ratio of the zinc aluminate ceramics, which are made from the solid state route powder, as determined by energy dispersive X-ray (EDX measurements) on polished surfaces is 0.99:2, consistent with the zinc deficient character of the starting powders.

The zinc deficiency is due to the volatile nature of zinc oxide (zinc oxide, $p_{Zn}=9\times10^{-4}$ Pa at 1000 °C;[33] aluminium oxide, $p_{Al}=4\times10^{-13}$ Pa [34]; magnesium oxide, $p_{Mg}=4\times10^{-18}$ Pa [34]). The large surface area and presence of a flow in the furnace increases the deficiency for the zinc aluminate prepared via the sol-gel method as compared to the material prepared via the solid state route. The lower concentration of zinc in the coprecipitated zinc aluminate is due to heating without the lid.

The NMR spectra of the zinc aluminate powders prepared via the solid state and coprecipitation are shown in Figs. 2 and 3, respectively. The presence of a peak at ~60 ppm indicates that there is some inversion present in all the powders. However, the size of the peak indicates that the amount of inversion is very small. Kashii et al.[30] found the same results, but they kept zinc aluminate at 900 °C for 40 h in contrast to 800 °C for 8 h used in this investigation. Furthermore, it is clear that there is no difference between the two preparation methods and that neither the temperature nor the calcining time does have a significant influence.

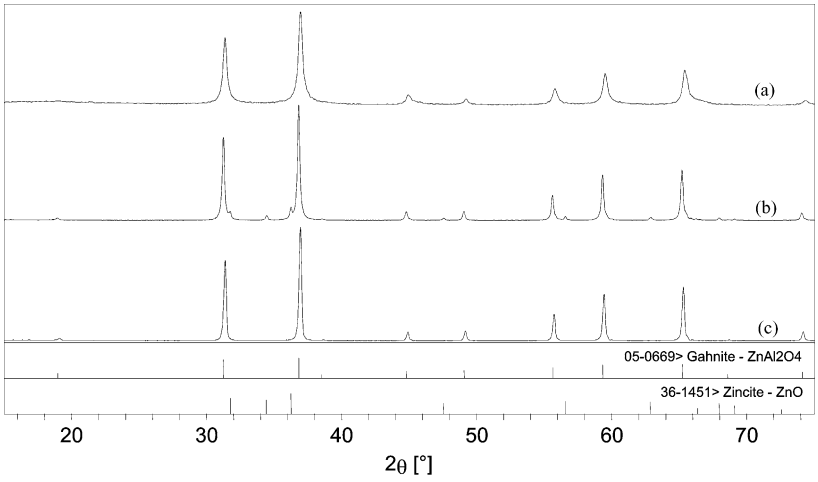

Fig. 1. XRD spectra of zinc aluminate powders prepared via (a) the sol-gel method (800 °C, 12 h), (b) coprecipitation (800°, 12 h) and (c) solid-state route (1000 °C, 8 h). Furthermore, the JCPDS files of gahnite (05-0669) and zincite (36-1451) are shown.

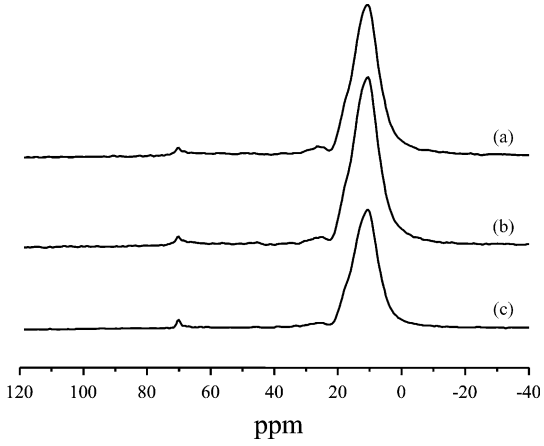

Fig. 2. ^{27}Al MAS NMR spectra of zinc aluminate prepared following the solid-state synthesis route at (a) 1000 °C for 8 h, (b) 800 °C for 8 h and (c) 800 °C for 12 h.

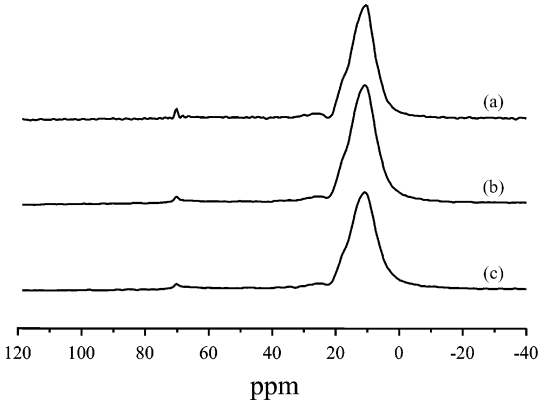

Fig. 3. ^{27}Al MAS NMR spectra of zinc aluminate prepared following the coprecipitation route at (a) 1000 °C for 8 h, (b) 800 °C for 8 h and (c) 800 °C for l2 h.

The NMR spectra of the zinc aluminate powder prepared by the sol-gel method are shown in Fig. 4 together with a spectrum of zinc aluminate prepared via the solid state synthesis route for comparison. In contrast to the other methods, the sol-gel method prepared zinc aluminate has a large degree of inversion. The normal degree of inversion, as obtained by the other methods, could not be reached after an additional reheating for 8 h at 1000 °C. This is in contrast with the results of Mathur et al.[14] who found a large degree of inversion at 600 °C, but a small degree at 1000 °C.

The large degree of inversion in the sol-gel prepared zinc aluminate cannot be attributed to the presence of aluminium cations with four or five oxygen atom surroundings at the surface, as zinc aluminate prepared via the sol-gel route has a large surface area.[35] The NMR experiments were performed in a quantitative manner, revealing that all aluminium cations are detected and that shielding of the bulk cations did not occur. This implies that the inversion is occurring in the bulk and is not an artefact of surface aluminium cations, since they form only a minor fraction of all the aluminium cations.

The NMR spectra have been measured on a largely zinc deficient zinc aluminate, which implies an excess of aluminium cations forming aluminium oxide. The absence of a second phase in XRD spectra suggests that a "solid solution" of the spinel phase of aluminium oxide (γ-alumina) and zinc aluminate has been formed resulting in the presence of a large amount of aluminium cations in tetrahedral interstices. In γ-alumina 25% of the aluminium cations are located at tetrahedral interstices[32] and therefore will contribute to the peak at 60 ppm. In order to determine the inversion parameter of pure zinc aluminate from these spectra, a correction to Eq. (1) for this γ-alumina contribution must be made. The inversion parameter for zinc deficient zinc alumina ($Zn_{1-y}Al_2O_{4-y}$) is given by:

$$x = \frac{2}{1 + (Al^{VI}/Al^{IV})} - \frac{1}{2}y \quad (2)$$

The first term on the right hand side of Eq. (2), for all powders prepared via the solid state route and coprecipitation, equals 0.04 ± 0.01 and for the sol-gel method 0.23 ± 0.02. Application of the correction for the zinc aluminate prepared via the solid state route ($y = 0.05$) and sol-gel method ($y = 0.52$) gives an inversion parameter of 0.015 and -0.01, respectively. However, a systematic error is present in estimating the inversion parameter from MAS-NMR spectra due to the location of some intensity in the spinning side bands and to the baseline correction. The results obtained are within the error range the same and it is concluded that the inversion parameter for of pure zinc aluminate is very small irrespective of the preparation method.

5.3. Elastic properties

The density of the sintered zinc aluminate tablets has been measured using the Archimedes' method with water as the displaceable fluid for densities higher than 90% and below 90% by the measuring the dimensions and weight of the tablet. The density as a function of the sintering temperature is shown in Fig. 5. The density increases with sintering temperature and remains constant at 93% from 1300 °C onwards.

Sidorov found that single phase zinc aluminate powder calcined at 1250 °C did not sinter without additives like TiO_2 up to 1650 °C.[15] However, Hong et al. found that single phase powder calcined at 1300 °C did sinter, but reached at 1400 °C a maximum density of 80%.[9] In this work, the zinc aluminate powder was calcined at 1000 °C, indicating that some zinc oxide is still present. This latter compound reacts during sintering and can contribute to an extra densification. However, since the average of the densities of zinc oxide (5.679 g cm^{-3}) and aluminium oxide (3.990 g cm^{-3}) is smaller that the density of zinc aluminate (4.611 g cm^{-3}), this reaction will leave pores and therefore a 100% density cannot be reached. The Young's modulus has been measured using the pulse–echo method as a function of density and is shown in Fig. 6. The absence of experimental data above a density of 95% makes it impossible to predict an accurate value for the zero porosity Young's modulus. However, an estimate can be made by linear extrapolation yielding 242 GPa.

5.4. Thermophysical properties

The heat capacity (C_p) of zinc aluminate powder has been measured using differential scanning calorimetry between 15 and 100 °C on zinc aluminate powder reheated up to 1400 °C for 8 h. The heat capacity at 300 K is 124 J mol^{-1} K^{-1}. The thermal diffusivity (a) of sintered zinc aluminate ceramics has been determined using the flash method on three 1.4 mm thick tablets with a density of 74, 91 and 94% ($T_{sinter} = 1250$, 1400 and 1600 °C, respectively) using the flash method[36,37] at different

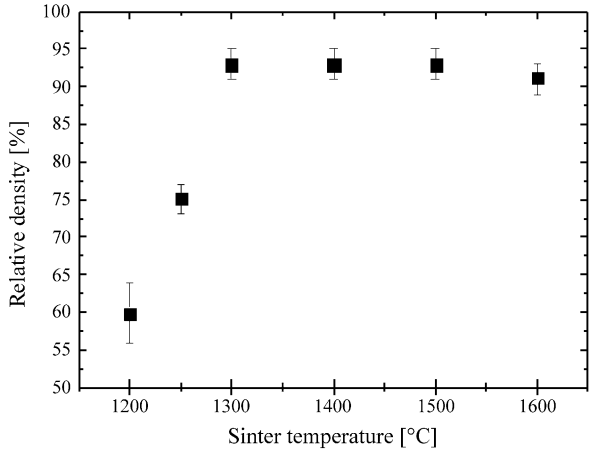

Fig. 5. Density as a function of sinter temperature of zinc aluminate uniaxially prepressed at 70 MPa.

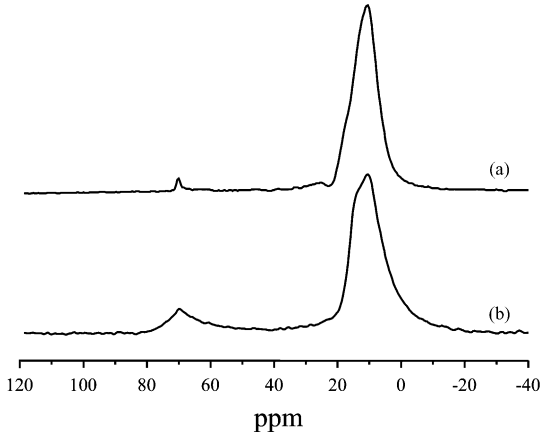

Fig. 4. ^{27}Al MAS NMR spectra of zinc atuminate prepared by (a) sol-gel synthesis and (b) solid-state synthesis for comparison.

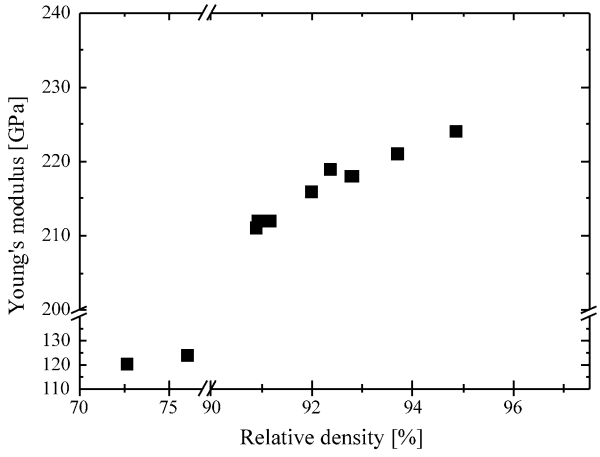

Fig. 6. Young's modulus of zinc aluminate as a function of density.

temperatures between room temperature and 250 °C. The thermal conductivity (κ) can be obtained from:

$$\kappa = a\rho C_p, \tag{3}$$

where ρ is the density (mol m^{-3}), which is for fully dense zinc aluminate ceramics 25 142 mol m^3, and ranges at room temperature from 12 to 14 W m^{-1} K^{-1} for the two highest densities.

Thermal conduction in ceramics predominantly takes place via lattice vibrations (i.e. phonon conductivity). It is being determined by lattice characteristics (intrinsic properties) and defects as impurities, grain boundaries and pores (extrinsic properties). At sufficiently high temperature, $T > \Theta_{D,r}/b$, where $\Theta_{D,r}$ is the reduced Debye temperature (Θ_D) and b is a constant ($\approx$2), the inverse of the thermal diffusivity is linearly related to the absolute temperature as given by:

$$\frac{1}{a} = \left(\frac{bA}{\Theta_{D,r}}\right)T + \left(B - \frac{A}{2}\right) = A'T + B', \tag{4}$$

where A is related to the phonon–phonon scattering processes (intrinsic lattice diffusivity), B is related to the phonon-scattering processes due to impurities, grain boundaries, etc., and $\Theta_{D,r}$ is the reduced Debye temperature defined as $\Theta_D/\sqrt[3]{n}$, where n is the number of atoms per primitive unit cell ($n = 14$ for zinc aluminate).[37] The values of A' and B' for different tablets investigated are obtained by a linear fit and shown in Table 1.

For the determination of the maximum thermal diffusivity and maximum thermal conductivity ($B = 0$),[37] the intercept at the inverse thermal diffusivity axis ($= A/2$) or the intercept at the temperature axis ($= \Theta_{D,r}/2b$) should be known in combination with the slope A' ($= bA/\Theta_{D,r}$). The estimated maximum thermal conductivity of the tablets investigated at 300 K are calculated using $\Theta_D = 896$ K as calculated from the phonon spectrum,[38] $n = 14$ and $b = 2$. The results are also shown in Table 1.

The three tablets investigated differ in porosity. This would imply a constant value for A', which only contains intrinsic diffusivity properties, and different values for B', which also contains influences due to pores. However, the values for A' differ somewhat, which imply that next to porosity the samples also differ in other aspects. In particular, the difference in sinter temperature might have influenced the pore shape and/or the composition to certain extent, since at high temperatures zinc can evaporate from the ceramic[39] although precautions have been taken to prevent it. The maximum achievable thermal conductivity at 300 K as estimated using the above described procedure is about 20–25 W m^{-1} K^{-1}. The large difference between the experimental values of 12–14 W m^{-1} K^{-1} and the above estimated are due to the large porosity. Such a difference is not uncommon: e.g. even for fully dense $MgSiN_2$ ceramics containing impurities $\sim$28 and $\sim$23 W m^{-1} K^{-1} are obtained for the maximum achievable and measured thermal conductivity, respectively.[37]

5.5. Dielectric properties

Two 0.5 mm thick parallel plate capacitors have been prepared from a tablet (1400 °C, 150 MPa) with a relative density of 90%. On these capacitors, round silver electrode areas of 12.566 mm^2 have been evaporated. Since the capacitors are not made of a fully dense polycrystalline material, the real part of the measured dielectric constants (k'_{meas}) is related to the real part of the single crystal dielectric constant (k') by:

$$k' = \left(\frac{3-\rho}{2\rho}\right)k'_{meas}, \tag{5}$$

where ρ is the relative density.[40]

The results are shown in Table 2. An accuracy of 10% is reached.

The polarizabiity (α) is the ability of ions or atoms to deform under an externally applied electric field and consists of space-charge, dipole, ionic and electronic components. The dielectric polarizability (α_D) is, on a microscopic level, related to the experimentally determined dielectric constant by the Clausius–Mosotti equation:

$$\alpha_D = \frac{1}{b}\left[V_m \frac{(k'-1)}{(k'+2)}\right], \tag{6}$$

where b is defined as $4\pi/3$, V_m the molar volume in Å^3 and k' is the real part of the complex dielectric constant, which is measured between 1 kHz and 10 MHz.[41–43] The dielectric polarizability is in this range only composed of the ionic and electronic components, where the electronic component itself is related to the refractive

Table 1
Thermal conductivity of zinc aluminate ceramics

Fit parameters temperature dependence [Eq. (4)]			R^2 (–)	Maximum
ρ (%)	A' (s m^{-2} K^{-1})	B' (s m^{-2})		($T = 300$ K) κ_{max} (W m^{-1} K^{-1})
74	754	316×10^3	0.9911	20
91	593	25.7×10^3	0.9913	25
94	679	41.1×10^3	0.98994	22

Table 2
Dielectric constant of zinc aluminate

	Frequency (MHz)	k'_{meas} (–)	k' (–)
k'_0	0.1	10.4	11.94
k'	1	9.23	10.60
tan δ		0.01815	
k'_∞	10	9.46	10.86

index n by the Lorenz–Lorentz equation:[44,45]

$$\alpha_e = \frac{1}{b}\left[V_m \frac{(n^2-1)}{(n^2+2)}\right]. \quad (7)$$

The dipole and space-charge components are not contributing to the polarizability at these frequencies. These mechanisms have a large relaxation time as compared to the frequencies used.

The dielectric polarizability of zinc aluminate calculated from $k' = 10.60$ is 12.06 Å^3 ($V_m = 66.08$ Å^3). The electronic polarizability, calculated from the refractive index $n = 1.7725$[46] is 6.57 Å^3, resulting in 5.49 Å^3 for the ionic polarizability.

The concept of additivity of polarizabilities is the assumption that the polarizability of a complex compound is the sum of the polarizabilities of the simpler compounds and which has been applied to both electronic and dielectric polarizabilities (see e.g. Ref. 47). Applying this additivity rule to zinc aluminate leads to a predicted dielectric polarizability of 11.76 Å^3 (ZnO: $\alpha_D = 4.13$ Å^3 Al_2O_3: $\alpha_D = 7.63$ Å^3).[48] The measured value of 12.06 Å^3 differs 2.5% from the predicted values, which is larger than the typical values of 0.5–1.0% for other aluminates, beryllates, borates, gallates, silicates and phosphates (references in Ref. 48), but can be explained by the large experimental error.

6. Conclusions

The structural, elastic, thermophysical and dielectric properties of zinc aluminate have been investigated. Zinc aluminate powders have been prepared at different temperatures, with different reaction times and via different preparation routes (solid-state, coprecipitation and sol-gel). Zinc deficient zinc aluminate has been made, which is due to the volatile nature of zinc oxide during calcining. Furthermore, it is established with quantitative MAS ^{27}Al NMR that the inversion parameter of pure zinc aluminate is very small.

Zinc aluminate ceramics have been made by sintering uniaxially prepressed tablets at temperatures above 1200 °C. A density of 93% is reached at 1300 °C and remains constant for higher sintering temperatures. A value of 242 GPa was estimated for the Young's modulus of fully dense material. The estimated dielectric constant of fully dense zinc aluminate ceramics is 10.60 and its polarizability is 12.06 Å^3. The prediction of this value from the polarizabiities of zinc and aluminium oxides using the oxide additivity rule gave a larger than typical difference of 2.5%.

The thermal conductivity of zinc aluminate is determined from the measured heat capacity (124 J mol^{-1} K^{-1}) and thermal diffusivity (4–5×10^{-6} m^2 s^{-1}), resulting in a value of 12–14 W m^{-1} K^{-1}. The maximum achievable thermal conductivity for pore and impurity free zinc aluminate ceramics has been estimated as 20–25 W m^{-1} K^{-1}.

Acknowledgements

M.M.R.M Hendrix and E.M. van Oers (Eindhoven University of Technology) are acknowledged for the XRD and NMR measurements, respectively, S. Tappe (RWTH Aachen University of Technology, Germany) for the dielectric measurements, A. Oberndorff-Laska (Eindhoven University of Technology) for the thermal diffusivity measurements and B. Norder (Delft University of Technology) for the heat capacity measurements.

References

1. Shioyama, T. K., *Alcohol Dehydration Employing a Zinc Aluminate Catalyst*. US Patent 4.260.845, 1981.
2. Le Pelier, F., Chaumette, P., Saussey, J., Bettahar, M. M. and Lavalley, J. C., Mol. Catal. A. *Chemical*, 1997, **122**, 131–139.
3. Szymansky, R., Travers, Ch., Chaumette, P., Courty, Ph. and Durand, D. In *Studies in Surface Science and Catalysis,* vol. 31, ed. B. Delmon, P. Grange, P. A. Jacobs and G. Poncelet. Elsevier, Amsterdam, 1987, pp. 739–748.
4. Cobb, L. R., *Preparation of Polymethylbenzenes*. US Patent 4.568.784, 1985.
5. Roesky, R., Weiguny, J., Bestgen, H. and Dingerdissen, U., Appl. Catal. A. *General*, 1999, **176**, 213–220.
6. Welch, M. B., *Zinc Aluminate Double Bond Isomerization Catalyst and Process for its Production*. US Patent 4.692.430, 1986.
7. Aguilar-RIos, G., Valenzuela, M., Salas, P., Armendáriz, H., Bosch, P., Del Toro, G., Silva, R., Bertin, V., Castillo, S., Ramirez-Solis, A. and Schifter, I., Hydrogen interactions and catalytic properties of platinum-tin supported on zinc aluminate. *Appl. Catal. A: General*, 1995, **127**, 65–75.
8. Escardino, A., Amorós, J. L., Gozalbo, A., Orts, M. J. and Moreno, A., Gahnite devitrification in ceramic frits: mechanism and kinetics. *J. Am. Ceram. Soc*., 2000, **83**, 2938–2944.
9. Hong, W.-S., De Jonghe, L. C., Yang, X. and Rahaman, M. N., Reaction sintering of ZnO–Al_2O_3. *J. Am. Ceram. Soc*., 1995, **78**, 3217–3224.
10. Keller, J. T., Agrawal, D. K. and McKinstry, H. A., Quantitative XRD studies of $ZnAl_2O_4$ (Spinet) synthesized by sol-gel and powder methods. *Adv. Ceram. Mater*., 1988, **3**, 420–422.
11. Zawadzki, M. and Wrzyszcz, J., Hydrothermal synthesis of nanoporous zinc aluminate with high surface area. *Mater. Res. Bull*., 2000, **35**, 109–114.
12. Valenzuela, M. A., Jacobs, J. P., Bosch, P., Reije, S., Zapata, B. and Brongersma, H. H., The influence of the preparation method

on the surface structure of $ZnA1_2O_4$. *Appl. Catal. A: General*, 1997, **148**, 315–324.
13. Kurihara, L. K. and Suib, S. L., Sol-gel synthesis of ternary metal oxides. 1. Synthesis and characterization of MAl_2O_4 (M = Mg, Ni, Co, Cu, Fe, Zn, Mn, Cd, Ca, Hg, Sr, and Ba) and $Pb_2A1_2O_5$. *Chem. Mater*., 1993, **5**, 609–613.
14. Mathur, S., Veith, M., Haas, M., Shen, H., Lecerf, N., Huch, V., Hüfner, S., Haberkorn, R., Beck, H. P. and Jilavi, M., Single source sol-gel synthesis of nanocrystalline $ZnAl_2O_4$: structural and optical properties. *J. Am. Ceram. Soc*., 2001, **84**, 1921–1928.
15. Sidorov, N. A., The sintering of gahnite (zinc aluminate), Trudy Khar'kov. *Politekh. Inst*., 1958, **17**, 251–255.
16. Kainarskii, I. S. and Sidorov, N. A., Dense porous and alkali-resistant ceramics from gahnite. *Ser. Khim.-Tekhnol*., 1957, **13**, 165–171.
17. Kainarskii, I. S. and Sidorov, N. A., Gahnite and its refractory properties. *Ogneupory*, 1958, **23**, 19–23.
18. Bragg, W. H., The structure of the spinel group of crystals. *Phil. Mag*., 1915, **30**, 305–315.
19. Nishikawa, S., Structure of some crystals of the spinel group. *Proc. Math. Phys. Soc. Tokyo*, 1915, **8**, 199–209.
20. Henry, N. F. M. and Lonsdale, K., ed., *International tables for X-ray crystallography,* vol. 1. Kynoch Press, Birmingham, UK, 1952.
21. Hahn, E. L., Spin echoes. *Phys. Rev*., 1950, **80**, 580–594.
22. Carr, H. Y. and Purcell, E. M., Effects of diffusion on the free precession in nuclear magnetic resonance experiments. *Phys. Rev*., 1954, **94**, 630–638.
23. Lynnworth, L. C., *Ultrasonic Measurements for Process Control*, 1st edn.. Academic Press, London, UK, 1989.
24. Cooley, R. F. and Reed, J. S., Equilibrium cation distribution in $NiAl_2O_4$, $CuAl_2O_4$ and $ZnAl_2O_4$ spinels. *J. Am. Ceram. Soc*., 1972, **55**, 395–398.
25. O'Neill, H.St.C. and Dollase, W. A., Crystal structures and cation distributions in simple spinels from powder XRD structural refinements: $MgCr_2O_4$, $ZnCr_2O_4$, Fe_3O_4 and the temperature dependence of the cation distribution in $ZnAl_2O_4$. *Phys. Chem. Minerals*, 1994, **20**, 541–555.
26. Lucchesi, S., Della Guista, A. and Russo, U., Cation distribution in natural Zn-aluminate spinels. *Miner. Mag*., 1998, **62**, 41–54.
27. Hill, R. J., Craig, J. R. and Gibbs, G. V., Systematics of the spinet structure type. *Phys. Chem. Miner*., 1979, **4**, 317–339.
28. Cormack, A. N., Lewis, G. V., Parker, S. C. and Catlow, C. R. A., On the cation distribution of spinels. *J. Phys. Chem. Solids*, 1988, **49**, 53–57.
29. Grimes, R. W., Anderson, A. B. and Heuer, A. H., Predictions of cation distributions in AB_2O_4 spinels from normalized ion energies. *J. Am. Chem. Soc*., 1989, **111**, 1–7.
30. Kashii, N., Maekawa, H. and Hinatsu, Y., Dynamics of cation mixing of $MgAl_2O_4$ and $ZnAl_2O_4$ spinel. *J. Am. Ceram. Soc*., 1999, **82**, 1844–1848.
31. Monrós, G., Carda, J., Tena, M. A., Escribando, P., Badenes, J. and Cordoncillo, E., Spinels from gelatin-protected gels. *J. Mater. Chem*., 1995, **5**, 85–90.
32. Levin, I. and Brandon, D., Metastable alumina polymorphs: crystal structures and transition sequences. *J. Am. Ceram. Soc*., 1998, **81**, 1995–2012.
33. Kodera, K., Kusunoki, I. and Shimizu, S., Dissociation pressures of various mettalic oxides. *Bull. Chem. Soc. Jpn*., 1968, **41**, 1039–1045.
34. Lou, V. L. K., Mitchell, T. E. and Heuer, A. H., Graphical displays of the thermodynamics of high-temperature gas-solid reactions and their application to oxidation of metals and evaporation of oxides. *J. Am. Ceram. Soc*., 1985, **68**, 49–58.
35. Valenzuela, M. A., Bosch, P., Aguilar-Rios, G. and Montoya Schifter, A., Comparison between sol-gel, coprecipitation and wet mixing synthesis of $ZnAl_2O_4$. *J. Sol-Gel Sci. Technol*., 1997, **8**, 107–110.
36. Parker, W. J., Jenkins, R. J., Butler, C. P. and Abbott, G. L., Flash method of determining thermal diffusivity, heat capacity and thermal conductivity. *J. Appl. Phys*., 1961, **32**, 1679–1684.
37. Bruls, R. J., Hintzen, H. T. and Metselaar, R., A new estimation method for the intrinsic thermal diffusivity/conductivity of non-metallic compounds: a case study for $MgSiN_2$, AlN and β-Si_3N_4 ceramics. *J. Am. Ceram. Soc*. (submitted for publication).
38. Fang, C. M., Loong, C.-K., de Wijs, G. A. and De With, G., Phonon spectrum of $ZnAl_2O_4$ spinet from in elastic neutron scattering and first-principles calculations. *Phys. Rev. B*, 2002, **66**, 144–301.
39. Inaba, H. and Matsui, T., Vaporaztion and diffusion of manganese-zinc ferrite. *J. Sot. State Chem*., 1996, **121**, 143–146.
40. Dunn, M. L., Effects of grain shape anisotropy, porosity, and microcracks on the elastic and dielectric constants of polycrystalline piezoelectric ceramics. *J. Appl. Phys*., 1995, **78**, 1533–1541.
41. Roberts, S., Dielectric constants and polarizabilities of ions in simple crystals and barium titanate. *Phys. Rev*., 1949, **76**, 1215–1220.
42. Roberts, S., A theory of dielectric polarization in alkali-halide crystals. *Phys. Rev*., 1950, **77**, 258–263.
43. Roberts, S., Polarizabilities of ions in perovskite-type crystals. *Phys. Rev*., 1951, **81**, 865–868.
44. Lorenz, H. A., Uber die Beziehung zwischen der Fortpflanzungsgeschwindigkeit de Lichtes und die Körperdichte. *Ann. Phys. Chem*., 1880, **9**, 641–645.
45. Lorentz, L., Uber die Refraktionskonstanten. *Ann. Phys. Chem*., 1880, **11**, 70–103.
46. Medenbach, O. and Shannon, R. D., Refractive indices and optical dispersion of 103 synthetic and mineral oxides and silicates measured by a small-prism technique. *J. Opt. Soc. Am. B*, 1997, **14**, 3299–3318.
47. Shannon, R. D. and Subramanian, M. A., Dielectric constants of chrysoberyl, spinel, phenacite and forsterite and the oxide additivity rule. *Phys. Chem. Min*., 1989, **16**, 747–751.
48. Shannon, R. D., Dielectric polarizabilities of ions in oxides and fluorides. *J. Appl. Phys*., 1993, **73**, 348–366.